

# Atomic structures at last: the ribosome in 2000

V Ramakrishnan\* and PB Moore†

Last year, atomic structures of the 50S ribosomal subunit from *Haloarcula marismortui* and of the 30S ribosomal subunit from *Thermus thermophilus* were published. A year before that, a 7.8 Å resolution electron density map of the 70S ribosome from *T. thermophilus* appeared. This information is revolutionizing our understanding of protein synthesis.

## Addresses

\*Medical Research Council Laboratory of Molecular Biology, Cambridge, UK; e-mail: ramak@mrc-lmb.cam.ac.uk

†Departments of Chemistry, and Molecular Biophysics and Biochemistry, Yale University, New Haven, CT 06520-8107, USA; e-mail: moore@proton.chem.yale.edu

Current Opinion in Structural Biology 2001, 11:144–154

0959-440X/01/\$ – see front matter

© 2001 Elsevier Science Ltd. All rights reserved.

## Abbreviations

EF-2 elongation factor 2  
EF-G elongation factor G  
EF-Tu elongation factor Tu  
rmsd root mean square deviation

## Introduction

The ribosome is the particle that catalyzes mRNA-directed protein synthesis in all organisms. It mediates the interactions between mRNAs and tRNAs on which the fidelity of translation depends and it contains the activity that catalyzes peptide bond formation. Prokaryotic ribosomes, which sediment at 70S, have molecular weights around  $2.5 \times 10^6$  and consist of two subunits, the larger of which, the 50S subunit, is about twice the mass of the smaller, the 30S subunit. Both are approximately two-thirds RNA by weight. The small subunit contains a single RNA roughly 1500 nucleotides in length, 16S rRNA, and single copies of each of about 20 different proteins. The large subunit contains a 2900-nucleotide RNA, 23S rRNA, an RNA of about 120 nucleotides, 5S rRNA, and 30–40 different proteins, depending on species. Eukaryotic ribosomes contain more components and are significantly bigger than prokaryotic ribosomes, but they resemble them both architecturally and in their *modus operandi*.

For the communities interested in translation and/or RNA, 2000 was an *annus mirabilis*. It was the year in which the first atomic-resolution crystal structures appeared for both the large and the small ribosomal subunits. Students of the ribosome had long labored in a world rich in sequence information, but poor in conformational information. This imbalance was now corrected. In addition, with the publication of these structures, the amount of atomic-resolution, three-dimensional RNA structure available for study increased roughly 10-fold and there was an equally dramatic expansion in the structural database for RNA–protein complexes. The world of the RNA biochemist had changed also.

This review covers the literature on the crystallography and electron microscopy of intact ribosomes and ribosomal subunits that appeared between May 1st 1999 and November 1st 2000. The literature on the structures of individual ribosomal components and ribosome subassemblies, which also expanded significantly in that period, is not evaluated. The best single source of information about the ribosome is a recent conference proceedings volume [1•]. It includes several articles about ribosome crystallography and electron microscopy that are not reviewed here because the results they describe have appeared in the primary literature.

## Crystallography of ribosomes and their subunits

### The origins of ribosome crystallography

In 1980, Yonath, Wittmann and co-workers [2] reported the first three-dimensional crystals of 50S ribosomal subunits; five years later, Yonath and co-workers [3,4] obtained the crystals of *Haloarcula marismortui* large ribosomal subunits that ultimately yielded the atomic structure of the large ribosomal subunit discussed below. The progenitors of the crystals of the 30S subunit and 70S ribosome from *Thermus thermophilus* that have now been solved were produced by Trakhanov *et al.* [5] and, shortly afterwards, similar crystals were reported by Yonath and co-workers [6]. Refinement of these crystals [7,8•] enabled both the Yonath and the Ramakrishnan groups to collect 30S subunit diffraction data beyond 3 Å resolution, and the Noller group [9••] to collect 70S ribosome data past 6 Å resolution.

If between 1980 and 2000 progress had been made only in ribosome crystallization, we would still be waiting for structures. Ribosome crystals posed challenges in the areas of data collection and crystallographic computation that could not have been met in 1980. By about 1995, however, improvements in area detectors, synchrotron light sources, computers and crystallographic software had opened the door to solving structures of ribosomal complexity. Two other important advances were the development of cryo-crystallography (reviewed in [10]), of which Yonath [11] was an early advocate, and tunable synchrotron sources, which made it possible to take full advantage of anomalous scattering [12]. At that point, the primary technical problem that had to be solved was finding a way to phase the diffraction patterns produced by ribosome crystals.

The first convincing evidence that the phase problem was tractable came in 1998 when a 9 Å resolution crystallographic electron density map of the *H. marismortui* 50S subunit was published that had right-handed, double-helical density corresponding to A-form RNA and a molecular envelope that clearly resembled electron microscopic images of the 50S subunit [13]. Two approaches to phasing

were used in that work. First, using electron microscopic reconstructions of the 50S subunit as starting models, phases were computed by molecular replacement, as virus crystallographers had done in the past [14]. Second, again following precedent [15,16], heavy atom cluster compounds were used to obtain experimental phases by isomorphous replacement. A third phasing strategy, used somewhat later, exploited the strong anomalous scattering produced by the LIII absorption edges of lanthanide ions and the hexamines of osmium and iridium, an approach used earlier for crystals of smaller proteins [17] and RNAs [18].

A second wave of breakthroughs came in 1999, when electron density maps of approximately 5 Å resolution were obtained for both subunits. Ribosomal components that had been solved to high resolution in isolation could be recognized and placed within these electron density maps [8\*,19\*]. In addition, partly because the 30S subunit is so well understood biochemically, the central domain and the long penultimate helix in the sequence of 16S rRNA were traced. Later that year, Yonath and co-workers [20] published a 4.5 Å resolution electron density map of the 30S subunit. Proteins S5 and S7 were placed in the electron density, and the 3' end of the 16S rRNA and epitopes on S11 and S13 were located using tagged heavy atoms.

1999 also saw the publication of a 7.8 Å resolution electron density map of the 70S ribosome complexed with mRNA and tRNA [9\*\*]. There are three tRNA-binding sites on the ribosome: the A (or aminoacyl) site, which binds the tRNA with the new amino acid to be added; the P (or peptidyl) site, which holds the tRNA with the nascent polypeptide chain; and the E (or exit) site, which binds the deacylated tRNA before its ejection from the ribosome. Electron densities for mRNA and tRNAs in the A, P and E sites were evident in this map, imaged at a resolution significantly higher than that achieved with electron microscopy thus far (see below). Apart from the information it directly provided about tRNA interactions with the ribosome, the structure was extremely useful in a functional analysis of the atomic structure of the 30S subunit, described below. In addition, the 70S map proves that crystallography can be done on whole 70S ribosomes in defined functional states, a fact of the utmost importance for future investigations.

#### Atomic structures of the 50S and 30S subunits

The breakthroughs of 1999 were exciting not so much because of the information they provided about ribosome structure, but because they indicated that the barriers that had prevented the determination of atomic-resolution ribosome structures for so long would shortly be overcome; in 2000, that expectation was fulfilled. The structure of the 50S subunit from *H. marismortui* has now been solved to 2.4 Å resolution [21\*\*] and two high-resolution structures have appeared for the 30S subunit from *Thermus thermophilus*, one from the Yonath group at 3.3 Å resolution [22\*\*] and the other from the Ramakrishnan group at 3.0 Å [23\*\*].

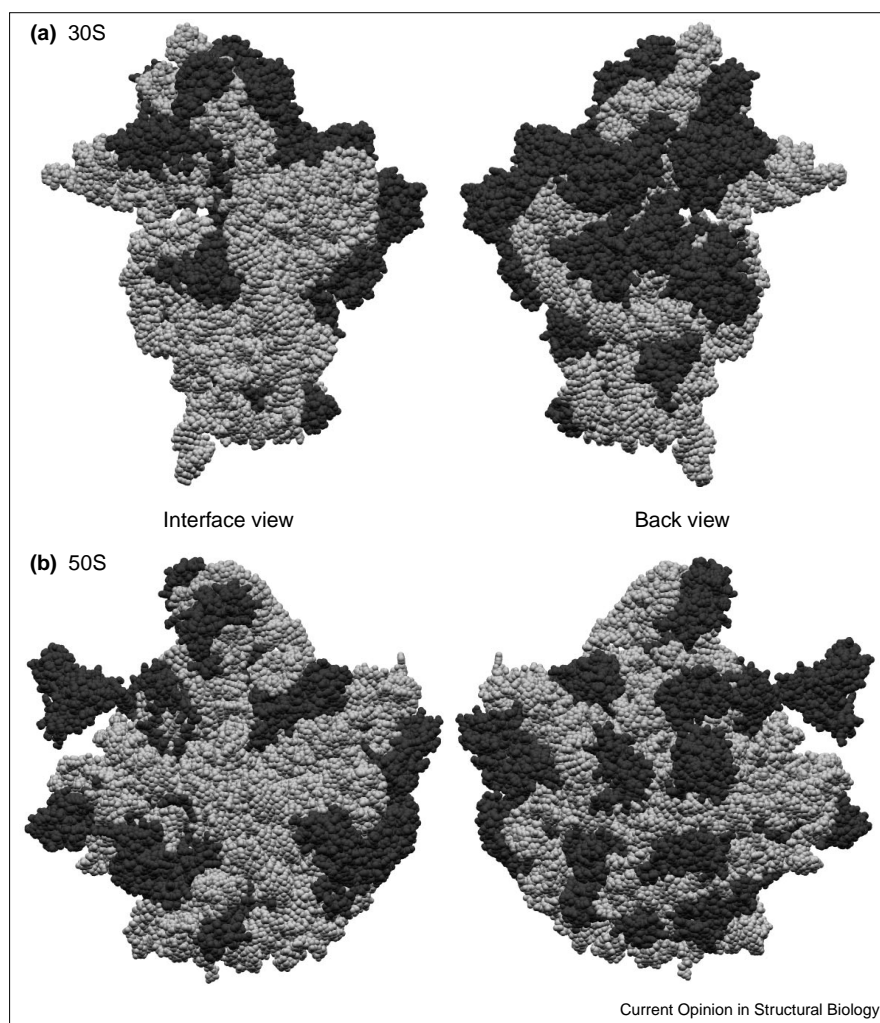
Superposition of the RNA backbones of the two 30S structures reveals that their RNA folds and global conformations are very similar. Thus, it is unlikely that one of these structures represents a more 'active' form of the 30S subunit than the other, contrary to previous claims [20,22\*\*]. Moreover, the crystal packing is similar in the two structures and the same as that reported earlier by the Ramakrishnan group [8\*], but different from that inferred previously by the Yonath group [24] on the basis of molecular replacement using a cryo-electron microscopy model. At the atomic level, however, there are significant differences. The structures differ in their level of completeness; the Ramakrishnan structure contains 51,737 atoms, whereas the Yonath structure contains 34,970. Most of this discrepancy is due to differences in the extent to which the electron density for proteins of previously unknown structure has been interpreted. The topologies assigned to many of these proteins are also incompatible. There are differences in the registry (and often the local structure) of the RNA in a number of regions; these regions account for about 300 nucleotides out of 1522. The rmsd between the phosphate atoms in the structures is 6.1 Å in these regions, compared with an rmsd of 3.6 Å for all the phosphate atoms in the RNA. These differences probably reflect the difficulties inherent in interpreting 3.3 Å resolution electron density maps, rather than genuine differences in conformation. Despite these differences, both papers agree on the global architecture and each offers additional unique insights into the 30S subunit.

#### Architectural generalities

Some generalities have emerged from the structures of the two subunits. First, the intersubunit interface of both subunits, especially the part that binds mRNA and tRNAs, is largely free of protein (Figure 1). Second, many proteins in both subunits have both a globular domain, which is generally found on the surface of the subunit, and long extensions that penetrate into the RNA and stabilize its tertiary structure; some proteins are devoid of a globular domain altogether, for example, S14 in the small subunit and L39e in the large subunit (Figure 2). Third, and quite surprisingly, the secondary structure motifs seen in the large rRNAs have almost all been seen before in smaller RNA structures. As the amount of RNA structure known at atomic resolution increased about 10-fold upon the publication of the structures of the two ribosomal subunits, this observation suggests that the repertoire of RNA secondary structure motifs is limited.

At the tertiary level, both 16S and 23S rRNA can be thought of as assemblies of helical elements connected by loops, which are often irregular extensions of helices. These structures are stabilized by interactions between helices, which include the minor-groove to minor-groove packing seen earlier in the group I intron structure [18], as well as less common motifs involving the insertion of a phosphate ridge into a minor groove and, occasionally, the use of an unpaired purine base to pack two helices perpendicularly with respect to each other. In many places, tertiary structure is stabilized by adenines inserted into the

Figure 1



Distribution of proteins and RNA in the (a) 30S and (b) 50S subunits. The dark gray shows protein and light gray shows RNA. The interface side, especially the part involved in interactions with mRNA and tRNA, is mostly protein-free in both subunits.

minor groove of helices that are distant in sequence. The adenines involved are often highly conserved.

A striking difference between the two subunits has to do with the relationship between the secondary structures of their RNAs and their overall morphology (Figure 3). In the 30S structure (Figure 3a), each of the large secondary structure domains of 16S rRNA forms a distinct morphological component of the subunit; the 5' domain forms the body, the central domain forms the platform, the 3' major domain forms the head and the 3' minor domain straddles the interface. In contrast, the six secondary structure domains of 23S rRNA (Figure 3b) are intricately interwoven in the 50S subunit to form a monolithic structure. This architectural difference may reflect a greater functional need for flexibility on the part of the small subunit.

#### Functional insights from crystallography

There are three central mechanistic questions concerning translation: how is peptide bond formation catalyzed; how are correct tRNAs discriminated from incorrect tRNAs;

and how are tRNAs and mRNA moved across the ribosome's active site at the end of each cycle of amino acid addition? Not surprisingly, the atomic structures of the subunits shed light on all of these issues.

The most decisive of the functional answers to emerge relates to the chemical nature of the peptidyl-transferase site, that is, the site on the 50S subunit where peptide bond formation occurs. Ever since the discovery of catalytic RNA, it has been suspected that rRNA might be responsible for the ribosome's peptidyl-transferase activity (e.g. see [25]). Using substrate analogs, such as that synthesized earlier by Yarus and co-workers [26], the Yale group [27••] located the peptidyl-transferase site crystallographically and showed that, indeed, it is composed entirely of RNA (Figure 4). The residues involved belong to the central loop of domain V in 23S rRNA. There can no longer be any doubt that the ribosome is a ribozyme.

Based on analog-binding data of this kind, a model for the mechanism of the peptidyl-transferase reaction has been

**Figure 2**

Gallery of protein structures from the (a) 30S and (b) 50S subunits. These show that many proteins have a globular domain and long extensions that would be disordered in isolated proteins. These extensions are often buried extensively in the RNA and are crucial for RNA folding. The globular domains of the proteins are shown in green and the regions that are highly extended are shown in red. Panel (b) is reproduced from [21••].

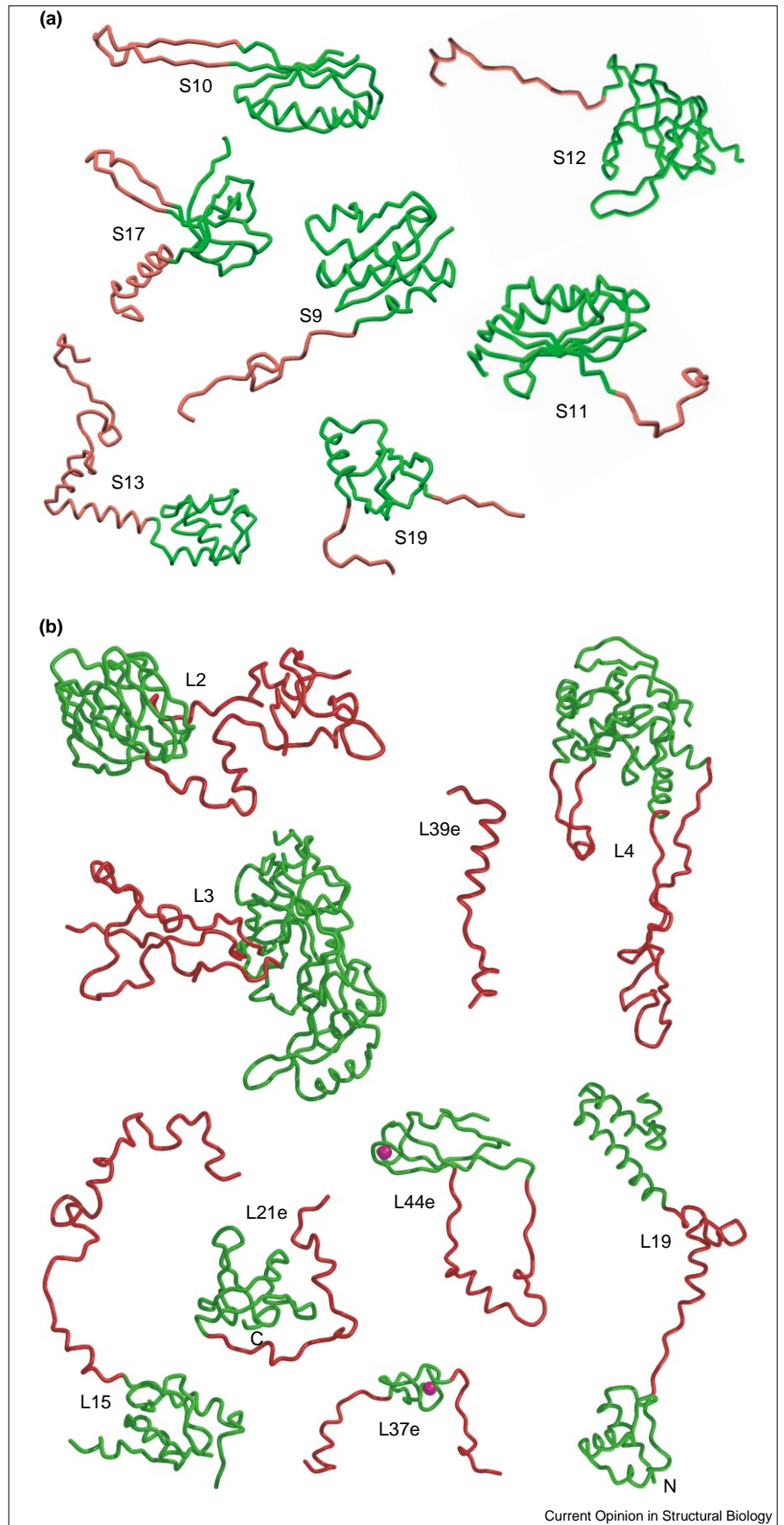
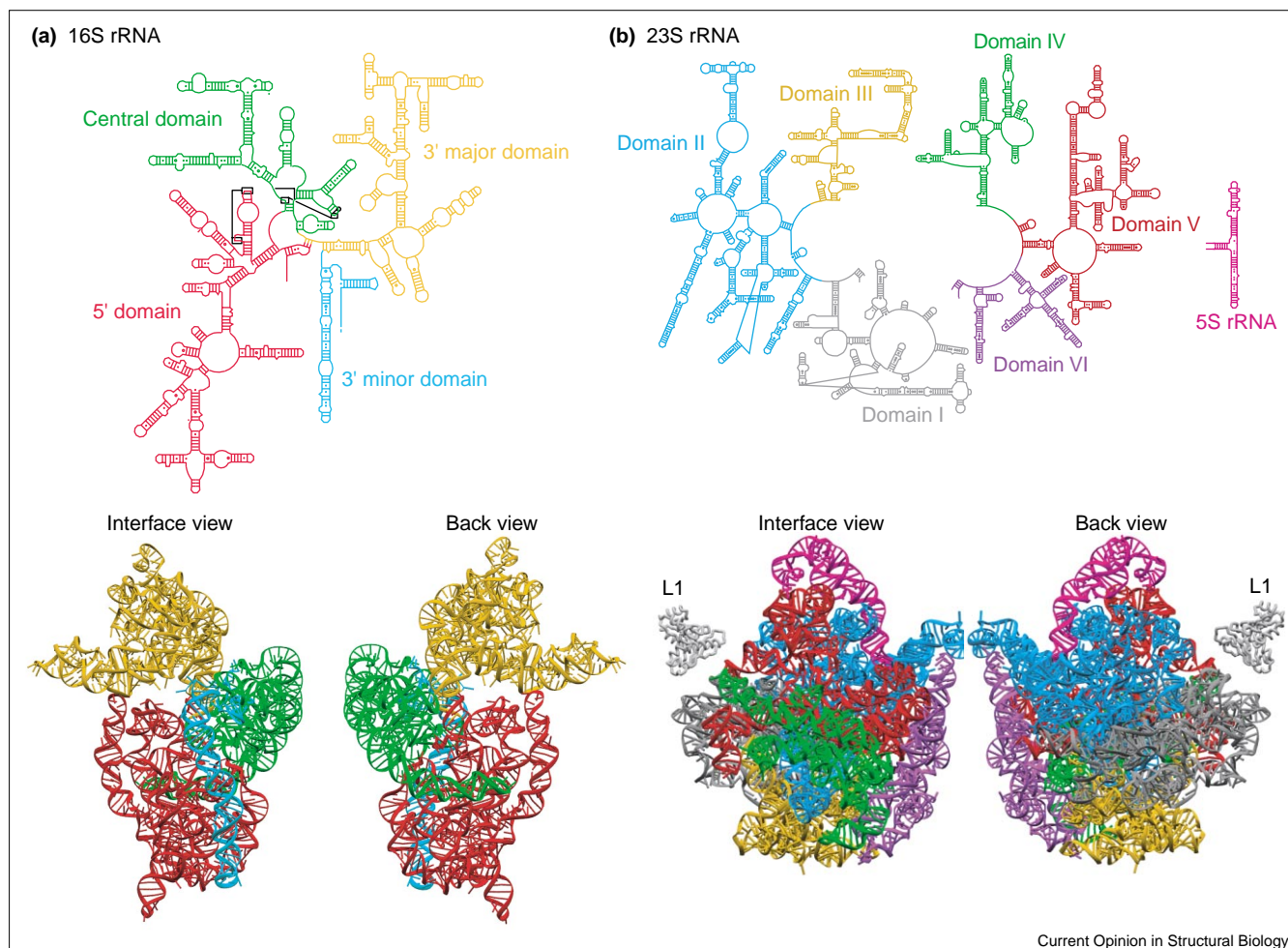


Figure 3



Current Opinion in Structural Biology

Secondary and tertiary structures of rRNA from the (a) 30S and (b) 50S subunits. These show a striking difference in the organization of the two large rRNAs. The secondary structure domains in 16S rRNA fold as distinct domains, whereas in 23S rRNA the secondary structure domains are intricately woven together in three dimensions. Each

domain has a similar color in the secondary and tertiary structures. Panel (a) is adapted from [23\*\*] and (b) is adapted from [21\*\*]. The line drawings for the secondary structure were originally adapted from the diagrams available on <http://www.rna.icmb.utexas.edu> (see also [58]).

advanced that proposes that peptide transfer is essentially the reverse of the serine deacylation reaction catalyzed by serine proteases. The entity that accelerates the reaction by acting as a general base, that is, the analog of His57 in chymotrypsin, is A2486 (A2451 in *Escherichia coli*). The  $pK_a$ s of nucleotide bases are normally too low to permit them to function this way, but, interestingly, a separate experiment done by Strobel and co-workers [28\*] has shown that this particular adenine has a  $pK_a$  close to 7.6, which is in the required range. This mechanistic proposal will unquestionably be tested experimentally in many different ways in the next few years. The Yale group [27\*\*] has also proposed that the unusual  $pK_a$  of A2486 reflects its indirect polarization by a nearby phosphate group that is inaccessible to solvent. This mechanism resembles the charge-relay mechanism invoked to explain the properties of the active sites of serine proteases.

The crystal structure of the large subunit also sheds further light on the polypeptide exit tunnel, the existence of which was finally proven by cryo-electron microscopy five years ago (see [1\*]). The tunnel lining is RNA over most of its length, with four of the six domains of 23S rRNA contributing. Tails from proteins L4 and L22, however, help form a constriction in the tunnel about a third of the way down from the peptidyl-transferase site [27\*\*]. Cross-linking studies performed by Choi and Brimacombe [29] provide beautiful evidence that nascent polypeptides do indeed traverse the tunnel as they are synthesized.

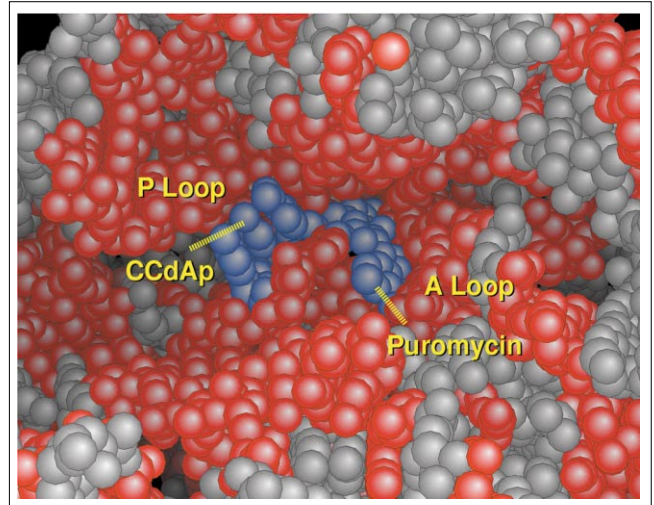
Functional analysis of the 30S subunit structure has been greatly aided by the fact that, in the particular crystal form studied, the 'spur', which is an RNA stem-loop that protrudes out from the bottom of the subunit and has a structure that resembles the anticodon stem-loop of a tRNA, is inserted into the P site of an adjacent 30S molecule [30\*\*].

Moreover, the 3' end of 16S rRNA appears to have folded back into the mRNA-binding cleft, providing a mimic for P- and E-site mRNA. The similarity of this interaction to the tRNA–mRNA–30S interaction that occurs during protein synthesis was confirmed by superimposing the 7.8 Å 70S structure, which contains both mRNA and tRNAs, onto the 30S structure. This exercise also revealed how tRNAs in the A and E sites interact with the small ribosomal subunit. The parts of the A and P sites on the 30S subunit consist largely of RNA, but, as observed in one of the two 30S structures [30\*\*], tendrils from S9 and S13 contact P-site-bound tRNA.

Additional insights have been gained from the structures obtained for the 30S subunit bound to the antibiotics spectinomycin, streptomycin and paromomycin [30\*\*]. Spectinomycin binds close to a pivot point between the head and body of the 30S subunit, where it interferes with the motions of the head that accompany translocation, consistent with its previously established role. Streptomycin appears to have a similar conformation-locking effect. In its presence, a conformation of the ribosome that is more error-prone, but has a higher affinity for tRNA, known as the *ram* conformation, is stabilized and the ribosome becomes less accurate in translation. The structure also explains the changes in RNA reactivity observed when the small subunit switches from the *ram* to the hyperaccurate or restrictive state, as well as the effects of mutations on the resistance and dependence of ribosomes on streptomycin.

The third antibiotic examined, paromomycin, sheds light on how the 30S subunit discriminates between cognate and near-cognate tRNAs (Figure 5). Paromomycin binds to an internal loop at the top of the long penultimate helix (H44) of 16S rRNA that contains the decoding site, in a manner that is largely consistent with earlier NMR data [31]. In the crystal structure, however, bases A1492 and A1493 are completely flipped out of the internal loop that is the drug's binding site, and A1493 does not form a base pair with A1408, as seen in the NMR structure. Both A1492 and A1493 are universally conserved and have been implicated in decoding by footprinting with A-site tRNA [32], as well as by biochemical experiments that show that they are essential for viability and are involved in hydrogen bonding with mRNA [33\*]. In the structure of the 30S subunit containing paromomycin [30\*\*], these bases are positioned so that they can form hydrogen bonds with both mRNA and tRNA across the minor groove surface of base pairs in the A-site codon–anticodon helix. Because it effectively senses the shape, width and potential for hydrogen bonds of the minor groove, this interaction should be very sensitive to base pairing geometry and, thus, could enable the ribosome to discriminate between correct base pairings and mismatches. In the absence of tRNA, these bases are largely stacked in helix 44. Normally, the energetic penalty for unstacking these two bases is 'paid for' by compensating interactions with the correct codon–anticodon helix. The binding of paromomycin pays the energetic cost of

Figure 4



The location in the 50S subunit of CCdAp–puromycin, an inhibitor of peptidyl-transferase activity that mimics the transition state. The figure shows that the peptidyl-transferase site consists entirely of RNA, proving that the ribosome is a ribozyme. RNA nucleotides that are more than 95% conserved are colored in red, all other nucleotides are shown in gray and the inhibitor itself is shown in blue. Reproduced from [27\*\*].

flipping out these bases, which should increase the relative binding affinity of near-cognate tRNAs and thereby increase the error rate, as observed.

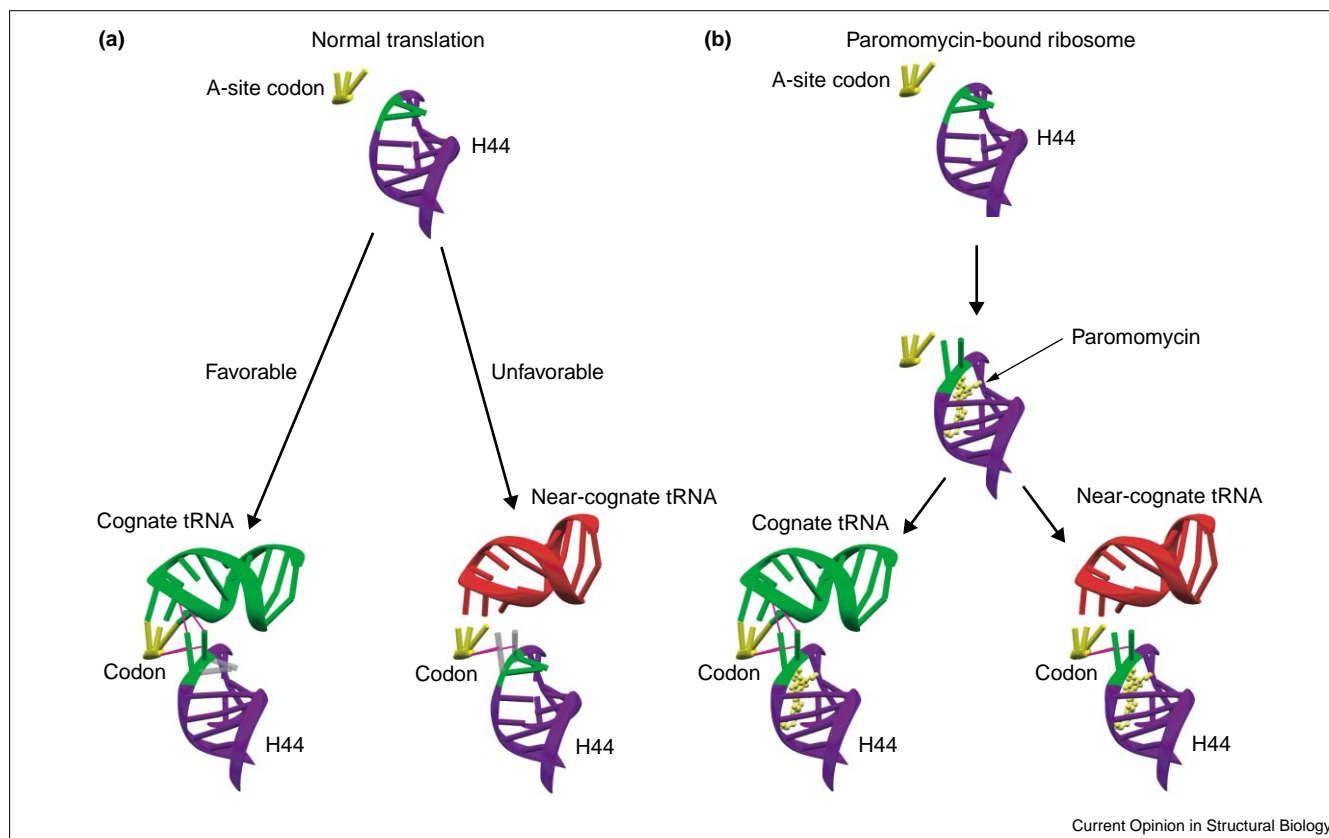
### Electron microscopy

Since 1995, the groups of Frank (Albany) and van Heel (London) have produced a remarkable series of medium-resolution images of the ribosome embedded in vitreous ice, obtained by three-dimensional reconstruction techniques from electron micrographs of individual ribosomal particles. The method is particularly well suited to the study of the different functional states of the ribosome because of the small quantities of material it requires. As the progress made in this area has been reviewed recently in this journal [34,35], only the more recent results will be reviewed here.

### Ribosome architecture

One of the most important goals of electron microscopists is improvement of the resolution of their reconstructions. Experience with two-dimensional and three-dimensional microcrystals shows that atomic-resolution structures can be obtained for macromolecules by electron microscopy, but this is yet to be achieved for single particles. Given the existence of atomic structures for both subunits, it would be unreasonable to expect that much will be learned about ribosome architecture if this is achieved, but the higher the resolution that can be routinely obtained, the easier it will be to understand the conformational changes in translating ribosomes revealed by electron microscopy (see below). We note, in passing, that the two groups engaged in ribosome electron microscopy do not compute the resolutions of their images the same way and that neither group does it the way that crystallographers do.

Figure 5



A scheme for how the initial steps in decoding would work in the 30S subunit and how paromomycin affects decoding. (a) In the normal situation, unstacking of bases A1492 and A1493 from an internal loop in helix 44 (H44) would only be favorable if compensating interactions could be made by hydrogen bonding with both mRNA and cognate tRNA across the minor groove of the codon–anticodon helix. This interaction would sense groove width and shape, and discriminate

against the distorted codon–anticodon helix formed with near-cognate or noncognate tRNAs. (b) Paromomycin, by binding in the internal loop, pays the energetic cost of flipping out these bases, thereby increasing the affinity of both cognate and near-cognate tRNAs. The pink lines represent potential hydrogen bonds formed by A1492 and A1493, shown in gray on helix 44. The bases are shown in gray in conformations that are unlikely.

The highest resolution claimed for a ribosome reconstruction so far is 7.5 Å, ascribed to a reconstruction of the large subunit from *E. coli*, based on the images of 16,000 particles. RNA helices can be recognized in the reconstruction and some ribosomal components can be located by matching high-resolution structures determined in isolation with features in the reconstruction [36\*]. Using this electron density map and the extensive body of biochemical information that relates to the organization of 23S rRNA, Brimacombe, van Heel and their co-workers [37\*] have generated a model for the large ribosomal subunit that includes all the helices of 23S and 5S rRNAs. By visual inspection, this model appears to be in rough agreement with the crystal structure of the 50S subunit.

More recently, a reconstruction of the 70S ribosome from *E. coli* was obtained, based on the images of 73,000 particles [38\*], and has an assigned resolution of 11.5 Å, in which RNA helices and protein shapes were also visible. Many of its features were assigned using information derived from the

5–5.5 Å resolution crystallographic electron density maps of the two subunits published in 1999 [8\*,19\*]. This reconstruction suggests that a significant conformational difference exists in the region that binds elongation factor Tu (EF-Tu) and elongation factor G (EF-G) on the surface of the large ribosomal subunit between the *E. coli* 70S ribosome and the same region in the *H. marismortui* 50S subunit. The Frank group [39,40] has developed two techniques that can help with the interpretation of less than atomic resolution electron microscopic images: a method for localizing rRNA sequences by the insertion of tRNA-sized sequences into rRNA that can then be visualized with electron microscopy [39] and a histogram-matching technique that can distinguish globular domains of proteins from RNA on the basis of density [40].

#### Conformational variability

Electron microscopy is ideally suited to the study of conformational changes during translation. The conformation of the small subunit is particularly variable because its ‘head’ is joined to the rest of the particle by a single RNA

helix and its position is not the same in the free subunit as it is in the 70S ribosome [41]. Of particular interest are conformational changes during translation as the ribosome switches from an error-prone or *ram* state to a hyperaccurate or restrictive state. This switch is associated with changes in base pairing within helix 27 of 16S rRNA [42]. A comparison of the structures of mutant 70S ribosomes that favor one state or the other shows that the conformation of both subunits changes from one state to the other [43•].

Electron microscopy studies have also addressed the way in which mRNA interacts with the ribosome during elongation. When the small subunit associates with the large, the head of the 30S subunit moves towards its shoulder to close a channel around the mRNA [44,45]. An exit channel is also formed by the closure of the platform and the head of the subunit, so the mRNA has to move through both channels during translation. The sizes of the entrance and exit channels vary reciprocally with the conformational state of the ribosome [43•,46•] and it was suggested that this could alternately clamp the mRNA or leave it free to move during translocation in a ratcheting motion. This idea has been elaborated upon by the Yonath group [22••]. They have analyzed their crystal structure of the 30S subunit to identify the RNA elements that form and close the entrance channel, and also identified an interconnected network of RNA helices that could allow a concerted movement of the subunit during translocation.

The large subunit is conformationally more conservative than the small subunit, but it too is flexible, as we have just seen. The most variable regions are its three protuberances: the L1 stalk, the central protuberance, which includes 5S rRNA, and the L7/L12 stalk, all of which vary with the functional state of the ribosome [34]. Strikingly, the L1 and L7/L12 stalks are also disordered in the crystal structure of the 50S subunit.

#### tRNA-binding sites

Since the 1960s, there has been evidence for two tRNA-binding sites on the ribosome, the A site, to which aminoacyl tRNAs bind at the time peptide bonds form, and the P site, where peptidyl tRNAs bind. In the mid-1980s, it became clear that there is a third site, the E site, to which deacylated tRNAs bind as they are discharged from the ribosome. One of the principal objectives of ribosome electron microscopists has been to determine the locations of these sites by visualizing tRNA molecules bound to the ribosome.

Of the three canonical sites, the most difficult to understand has been the E site, primarily because the interactions of deacylated tRNAs with the ribosome are sensitive to ionic conditions. Under conditions used classically for *in vitro* protein synthesis, deacylated tRNA binds to the ribosome in the same way as peptidyl tRNA, that is, it binds to the P site on both subunits. When buffers that contain polyamines are used, however, the CCA arm of deacylated tRNA binds to the large subunit at a position

well towards the L1 side of the P site, but its anticodon arm remains bound to the decoding center of the small subunit, in roughly the P site [34]. An analysis of tRNA interactions with the ribosome by the Frank group [47••], based on both their observations and the observations of others, indicates that deacylated tRNAs can bind to (at least) one other E-type site as they leave the ribosome, the so-called E2 site. The anticodon arm of tRNA bound to the E2 site is far from the decoding center of the small subunit.

A-site binding also appears to be more complicated than originally thought. Recent images from the Frank group [47••] suggest that tRNAs in the A site move slightly when peptide bond formation occurs. It could be that the motion detected corresponds to the shift of the acceptor stem of the tRNA that has just delivered its amino acid from the A-site region of the peptidyl-transferase site to the P-site region of the peptidyl-transferase site that the hybrid-states model for elongation posits must follow peptide bond formation [48]. The movement is greatest at the CCA end (on the large ribosomal subunit) and, after it has occurred, the CCA end of an A-site tRNA overlaps with the CCA end of a P-site tRNA [47••].

As first proposed many years ago, there is a fourth tRNA site on the ribosome that is functionally distinct from all the others — the site where aminoacyl tRNAs are delivered to the ribosome by EF-Tu. It barely overlaps with the A site [49]. The anticodon arm of a tRNA in this site extends into the decoding region of the small subunit, close to where the anticodons of tRNAs bound to the A site are found. However, instead of being oriented with its axis roughly normal to the interface surface of the small subunit, as it is for A-site-bound tRNAs, the axis of the anticodon arm is approximately parallel to that surface and the acceptor stem of the molecule interacts with the large subunit, close to the factor-binding site, instead of extending into the active site canyon of the large subunit towards the peptidyl-transferase center. The movement required to get an aminoacyl tRNA from its site of delivery to the A site is enormous. How do ribosome-bound tRNAs make that movement without dissociating from the ribosome? What, if anything, does this movement have to do with proofreading, which must occur at about the same stage in the elongation cycle?

The P site seems to be the only tRNA-binding site on whose position all parties agree and it seems the site least affected by changes in ionic conditions. It is comforting that the information about tRNA-binding sites derived from the crystal structure of the 70S ribosome [9••] is in reasonably good agreement with the information obtained by electron microscopy, but the electron microscopic data make it clear that a lot more work will have to be done before we fully understand how tRNAs work themselves across the subunit interface of the ribosome during elongation.

#### Elongation factor G

Following the addition of each amino acid to a growing polypeptide chain, a peptidyl tRNA in the A site must be

moved to the P site, a deacylated tRNA in the P site must move to the E site and mRNA must advance three nucleotides. All of these motions occur in a single concerted step called translocation, which is catalyzed by EF-G in prokaryotes and by elongation factor 2 (EF-2) in eukaryotes. As we shall see, translocation is as puzzling structurally as the EF-Tu-mediated binding of tRNAs to the A site.

Our understanding of the biochemistry of translocation has been transformed by experiments done by Wintermeyer, Rodnina and their co-workers over the past several years (reviewed in [50]). Their data suggest that the latent GTPase activity of EF-G•GTP is activated before translocation occurs, just as soon as it binds to the ribosome, probably as a result of its interaction with ribosomal protein L12. Translocation itself appears to be driven by conformational changes in EF-G that follow the dissociation of inorganic phosphate ( $P_i$ ) from the EF-G•GDP• $P_i$ -ribosome complex. It is only just before dissociation of the EF-G-ribosome complex that EF-G•GDP becomes associated with the sarcin-ricin loop of 23S rRNA in the large ribosomal subunit, the integrity of which is known to be critical for most factor interactions on the ribosome. The release of inorganic phosphate and the translocation of tRNAs both proceed at greatly reduced rates in the presence of thiostrepton, which arrests elongation entirely before the binding of EF-G to the sarcin-ricin loop. Fusidic acid, the other classic inhibitor of translocation, prevents the dissociation of EF-G from the ribosome following its association with the sarcin-ricin site.

Following the determination of the structure of the 70S ribosome bound to EF-G as a complex with GDP and fusidic acid [51], a number of functional states of the ribosome with EF-G have been studied. Reconstructions performed by the van Heel group in collaboration with the group of Rodnina and Wintermeyer [52••] have been interpreted as indicating that, when EF-G•GTP first interacts with the ribosome, it binds with its GTPase domain contacting the L7/L12 stalk of the 50S subunit and its fourth domain interacting with the 30S subunit in the region between its head and its body. Following GTP hydrolysis, translocation occurs and, in the process, EF-G appears to lose contact with the L7/L12 stalk, rotating about 90° so that domain four can enter the space between the two subunits, where it appears to contact the A site on the small subunit. Only when the translocation complex is trapped using fusidic acid can EF-G be seen bound to the ribosome associated with the sarcin-ricin loop in about the same orientation as the EF-Tu-tRNA complex when it is ribosome-bound. Significant rearrangements of the positions of the five domains of EF-G appear to accompany this process. The questions this sequence of events raise are similar to those posed by aminoacyl tRNA delivery. How can a macromolecule such as EF-G bind to the ribosome in two completely different ways and do anything useful as it makes its way from one binding mode to the other?

Frank and co-workers [53••] have also examined ribosome-EF-G complexes, but they have not looked at all the complexes studied by van Heel, Rodnina and Wintermeyer, which makes it difficult to compare results. The two groups agree that EF-G undergoes substantial conformational changes during translocation and Frank's group has devised a method for characterizing the states that preserves intradomain conformations as far as possible [54]. The two groups also agree about the way EF-G interacts with the ribosome in the presence of fusidic acid, the only complex they both have characterized recently. The complex the Frank group has examined, which the van Heel group has not, is the one formed when EF-G binds to the ribosome in the presence of a nonhydrolyzable GTP analog, GMPPCP. Based on the Wintermeyer and Rodnina scheme for translocation, one might have guessed that, in the presence of GMPPCP, EF-G would bind to the ribosome with its GTPase domain interacting with the L7/L12 stalk and domain four touching the small subunit in the region between its head and its body, that is, it would be trapped in the first of the states visualized by van Heel's group [52••]. This is not the case. The position of EF-G in this complex is similar to that seen in fusidic-acid-stabilized complexes, consistent with the biochemical observation that, in the presence of nonhydrolyzable GTP analogs, EF-G molecules will catalyze a single translocation event. The two complexes are not identical, however. They differ in the conformation adopted by the L7/L12 stalk in the large subunit. Taken by themselves, these findings suggest that EF-G need bind to the ribosome in only one way, which would be a relief if true, but models for translocation that simple may not be compatible with the kinetic data of Rodnina, Wintermeyer and co-workers [50]. Clearly, further experiments will have to be done for one to feel secure that translocation has been properly understood.

Frank and co-workers [55] have also imaged EF-2, the eukaryotic homolog of EF-G, bound to the yeast 80S ribosome in the presence of sordarin at 17.5 Å resolution. Sordarin has effects on eukaryotic translation that resemble those fusidic acid has on prokaryotic translation, but there are data suggesting that they do not act in exactly the same way. Nevertheless, in the presence of sordarin, EF-2 appears to bind to the yeast ribosome at the site that is the eukaryotic homolog of the site EF-G occupies when it binds to the *E. coli* ribosome in the presence of fusidic acid and it is oriented relative to the ribosome in much the same way. The Frank group [56] has also visualized initiation factor 3 bound to the small ribosomal subunit.

## Conclusions

The atomic structures of the two ribosomal subunits constitute an important first step towards the ultimate goal, which is to understand ribosome function in atomic detail. Many years of work will be required before that goal is reached, but the use of these structures, in conjunction with images obtained by electron microscopy, is certain to speed progress.

## Update

The structure of the 30S subunit in complex with the antibiotics tetracycline, pactamycin and hygromycin B [59] and with initiation factor IF1 [60] have also appeared recently. Tetracycline appears to bind mainly in the A site, where it can directly interfere with tRNA binding, but not necessarily with the binding of the EF-Tu•GTP complex. IF1 also binds in the A site of the ribosome in a manner that would preclude simultaneous tRNA binding. It also induces significant conformational changes in the 30S subunit that could be related to its role in initiation and shows how local conformational changes could be transmitted to domains of the 30S subunit.

## Acknowledgements

We thank Ditlev E Brodersen and William M Clemons Jr for producing the new or adapted figures in this paper. All figures were made using RIBBONS [57].

## References and recommended reading

Papers of particular interest, published within the annual period of review, have been highlighted as:

- of special interest
- of outstanding interest

1. Garrett RA, Douthwaite SR, Lijias A, Matheson AT, Moore PB, Noller HF (Eds): *The Ribosome. Structure, Function, Antibiotics and Cellular Interactions*. Washington, DC: ASM Press; 2000.
- Until the successor volume to this one is produced by the ribosome community, this book will be the best single reference for those interested in understanding the state of the ribosome field.
2. Yonath A, Mussig J, Tesche B, Lorenz S, Erdmann VA, Wittmann HG: **Crystallization of the large ribosomal subunits from *Bacillus stearothermophilus***. *Biochem Int* 1980, 1:428-435.
3. Shevack A, Gewitz HS, Hennemann B, Yonath A, Wittmann HG: **Characterization and crystallization of ribosomal particles from *Halobacterium marismortui***. *FEBS Lett* 1985, 184:68-71.
4. von Böhlen K, Makowski I, Hansen HAS, Bartels H, Berkovitch-Yellin Z, Zaytzev-Bashan A, Meyer S, Paulke C, Franceschi F, Yonath A: **Characterization and preliminary attempts for derivatization of crystals of large ribosomal subunits from *Haloarcula marismortui* diffracting to 3 Å resolution**. *J Mol Biol* 1991, 222:11-15.
5. Trakhanov SD, Yusupov MM, Agalarov SC, Garber MB, Ryazantsev SN, Tischenko SV, Shirokov VA: **Crystallization of 70 S ribosomes and 30 S ribosomal subunits from *Thermus thermophilus***. *FEBS Lett* 1987, 220:319-322.
6. Glotz C, Müssig J, Gewitz HS, Makowski I, Arad T, Yonath A, Wittmann HG: **Three-dimensional crystals of ribosomes and their subunits from eu- and archaeobacteria**. *Biochem Int* 1987, 15:953-960.
7. Yonath A, Harms J, Hansen HA, Bashan A, Schlunzen F, Levin I, Koelln I, Tocilj A, Agmon I, Peretz M *et al.*: **Crystallographic studies on the ribosome, a large macromolecular assembly exhibiting severe nonisomorphism, extreme beam sensitivity and no internal symmetry**. *Acta Crystallogr* 1998, A54:945-955.
8. Clemons WM Jr, May JLC, Wimberly BT, McCutcheon JP, Capel M, Ramakrishnan V: **Structure of a bacterial 30S ribosomal subunit at 5.5 Å resolution**. *Nature* 1999, 400:833-840.
- This work allowed placement of known components in an intermediate-resolution map of the 30S subunit. It also elucidated the fold of the entire central domain of 16S rRNA.
9. Cate JH, Yusupov MM, Yusupova GZ, Earnest TN, Noller HF: **X-ray crystal structures of 70S ribosome functional complexes**. *Science* 1999, 285:2095-2104.
- This paper sheds light on tRNA and mRNA binding to the ribosome, and paves the way for future studies on the whole ribosome and its functional complexes by crystallography.
10. Garman E: **Cool data: quantity AND quality**. *Acta Crystallogr* 1999, D55:1641-1653.
11. Hope H, Frolow F, von Böhlen K, Makowski I, Kratky C, Halfon Y, Danz H, Webster P, Bartels KS, Wittmann HG, Yonath A: **Cryocrystallography of ribosomal particles**. *Acta Crystallogr* 1989, B45:190-199.
12. Phillips JC, Wlodawer A, Goodfellow JM, Watenpaugh KD, Sieker LC, Jensen LH, Hodgson KO: **Applications of synchrotron radiation to protein crystallography. II. Anomalous scattering, absolute intensity and polarization**. *Acta Crystallogr* 1977, A33:445-455.
13. Ban N, Freeborn B, Nissen P, Penczek P, Grassucci RA, Sweet R, Frank J, Moore PB, Steitz TA: **A 9 Å resolution X-ray crystallographic map of the large ribosomal subunit**. *Cell* 1998, 93:1105-1115.
14. Jack A, Harrison SC, Crowther RA: **Structure of tomato bushy stunt virus. II. Comparison of results obtained by electron microscopy and X-ray diffraction**. *J Mol Biol* 1975, 97:163-172.
15. O'Halloran TV, Lippard SJ, Richmond TJ, Klug A: **Multiple heavy-atom reagents for macromolecular X-ray structure determination. Application to the nucleosome core particle**. *J Mol Biol* 1987, 194:705-712.
16. Andersson I, Knight S, Schneider G, Lindqvist Y, Lundqvist T, Brändén C-I, Lorimer GH: **Crystal structure of the active-site of ribulose-bisphosphate carboxylase**. *Nature* 1989, 337:229-234.
17. Weis WI, Kahn R, Fourme R, Drickamer K, Hendrickson WA: **Structure of the calcium-dependent lectin domain from a rat mannose-binding protein determined by MAD phasing**. *Science* 1991, 254:1608-1615.
18. Cate JH, Gooding AR, Podell E, Zhou K, Golden BL, Kundrot CE, Cech TR, Doudna JA: **Crystal structure of a group I ribozyme domain: principles of RNA packing**. *Science* 1996, 273:1678-1685.
19. Ban N, Nissen P, Hansen J, Capel M, Moore PB, Steitz TA: **Placement of protein and RNA structures into a 5 Å-resolution map of the 50S ribosomal subunit**. *Nature* 1999, 400:841-847.
- An intermediate-resolution structure of the 50S subunit that allowed placement of components of known structure is described.
20. Tocilj A, Schlunzen F, Janell D, Gluhmann M, Hansen HA, Harms J, Bashan A, Bartels H, Agmon I, Franceschi F, Yonath A: **The small ribosomal subunit from *Thermus thermophilus* at 4.5 Å resolution: pattern fittings and the identification of a functional site**. *Proc Natl Acad Sci USA* 1999, 96:14252-14257.
21. Ban N, Nissen P, Hansen J, Moore PB, Steitz TA: **The complete atomic structure of the large ribosomal subunit at 2.4 Å resolution**. *Science* 2000, 289:905-920.
- The title says it all. It will serve as a reference for years to come.
22. Schlunzen F, Tocilj A, Zarivach R, Harms J, Gluehmann M, Janell D, Bashan A, Bartels H, Agmon I, Franceschi F, Yonath A: **Structure of functionally activated small ribosomal subunit at 3.3 angstroms resolution**. *Cell* 2000, 102:615-623.
- A near-atomic structure of the 30S subunit that makes interesting points about elements involved in mRNA binding and movement.
23. Wimberly BT, Brodersen DE, Clemons WMJ, Morgan-Warren R, von Rhein C, Hartsch T, Ramakrishnan V: **Structure of the 30S ribosomal subunit**. *Nature* 2000, 407:327-339.
- A complete atomic structure of the 30S subunit that, like its 50S counterpart [21••], will serve as a reference for years to come.
24. Harms J, Tocilj A, Levin I, Agmon I, Stark H, Kolln I, van Heel M, Cuff M, Schlunzen F, Bashan A *et al.*: **Elucidating the medium-resolution structure of ribosomal particles: an interplay between electron cryo-microscopy and X-ray crystallography**. *Structure Fold Des* 1999, 7:931-941.
25. Noller HF, Hoffarth V, Zimniak L: **Unusual resistance of peptidyl transferase to protein extraction procedures**. *Science* 1992, 256:1416-1419.
26. Welch M, Chastang J, Yarus M: **An inhibitor of ribosomal peptidyl transferase using transition-state analogy**. *Biochemistry* 1995, 34:385-390.
27. Nissen P, Hansen J, Ban N, Moore PB, Steitz TA: **The structural basis of ribosome activity in peptide bond synthesis**. *Science* 2000, 289:920-930.
- The authors have unambiguously established that the ribosome is a ribozyme and propose a mechanism for peptidyl-transferase activity.
28. Muth GW, Ortoleva-Donnelly L, Strobel SA: **A single adenosine with a neutral pKa in the ribosomal peptidyl transferase center**. *Science* 2000, 289:947-950.
- This paper shows that the specific adenine of 23S rRNA that is suggested to be involved in peptidyl-transferase activity [27••] has its pK<sub>a</sub> shifted to a value that is compatible with the proposed mechanism.

29. Choi KM, Brimacombe R: **The path of the growing peptide chain through the 23S rRNA in the 50S ribosomal subunit: a comparative cross-linking study with three different peptide families.** *Nucleic Acids Res* 1998, **26**:887-895.
30. Carter AP, Clemons WMJ, Brodersen DE, Morgan-Warren R, Wimberly BT, Ramakrishnan V: **Functional insights from the structure of the 30S ribosomal subunit and its interaction with antibiotics.** *Nature* 2000, **407**:340-348.
- This paper describes the tRNA- and mRNA-binding sites on the 30S subunit in atomic detail and the structural basis for the actions of spectinomycin, streptomycin and paromomycin, the last of which suggests a concrete model for the first step in decoding.
31. Fourmy D, Recht MI, Blanchard SC, Puglisi JD: **Structure of the A site of *Escherichia coli* 16S ribosomal RNA complexed with an aminoglycoside antibiotic.** *Science* 1996, **274**:1367-1371.
32. Moazed D, Noller HF: **Binding of tRNA to the ribosomal A and P sites protects two distinct sets of nucleotides in 16 S rRNA.** *J Mol Biol* 1990, **211**:135-145.
33. Yoshizawa S, Fourmy D, Puglisi JD: **Recognition of the codon-anticodon helix by ribosomal RNA.** *Science* 1999, **285**:1722-1725.
- Biochemical evidence that two critical adenines in the 30S subunit are both essential and involved in decoding by hydrogen bonding to mRNA.
34. Agrawal RK, Frank J: **Structural studies of the translational apparatus.** *Curr Opin Struct Biol* 1999, **9**:215-221.
35. van Heel M: **Unveiling ribosomal structures: the final phases.** *Curr Opin Struct Biol* 2000, **10**:259-264.
36. Matadeen R, Patwardhan A, Gowen B, Orlova EV, Pape T, Cuff M, Mueller F, Brimacombe R, van Heel M: **The *Escherichia coli* large ribosomal subunit at 7.5 Å resolution.** *Structure Fold Des* 1999, **7**:1575-1583.
- This paper describes the results of an attempt to push electron microscopic reconstructions of ribosomes to the highest possible resolution.
37. Mueller F, Sommer I, Baranov P, Matadeen R, Stoldt M, Wohnert J, Gorchach M, van Heel M, Brimacombe R: **The 3D arrangement of the 23 S and 5 S rRNA in the *Escherichia coli* 50 S ribosomal subunit based on a cryo-electron microscopic reconstruction at 7.5 Å resolution.** *J Mol Biol* 2000, **298**:35-59.
- A model for the large ribosomal subunit is described. Comparison of this model with an atomic-resolution crystallographic structure of the large ribosomal subunit will enable the reader to evaluate how accurately macromolecular structures can be understood when intermediate-resolution electron density maps are interpreted with the aid of extensive biochemical data.
38. Gabashvili IS, Agrawal RK, Spahn CM, Grassucci RA, Svergun DI, Frank J, Penczek P: **Solution structure of the *E. coli* 70S ribosome at 11.5 Å resolution.** *Cell* 2000, **100**:537-549.
- Another landmark on the way to electron microscopic reconstructions of the ribosome that have resolutions high enough that their features can be unambiguously interpreted at atomic resolution.
39. Spahn CM, Grassucci RA, Penczek P, Frank J: **Direct three-dimensional localization and positive identification of RNA helices within the ribosome by means of genetic tagging and cryo-electron microscopy.** *Structure Fold Des* 1999, **7**:1567-1573.
40. Spahn CM, Penczek PA, Leith A, Frank J: **A method for differentiating proteins from nucleic acids in intermediate-resolution density maps: cryo-electron microscopy defines the quaternary structure of the *Escherichia coli* 70S ribosome.** *Structure Fold Des* 2000, **8**:937-948.
41. Gabashvili IS, Agrawal RK, Grassucci R, Frank J: **Structure and structural variations of the *Escherichia coli* 30S ribosomal subunit as revealed by three-dimensional cryo-electron microscopy.** *J Mol Biol* 1999, **286**:1285-1291.
42. Lodmell JS, Dahlberg AE: **A conformational switch in *Escherichia coli* 16S ribosomal RNA during decoding of messenger RNA.** *Science* 1997, **277**:1262-1267.
43. Gabashvili IS, Agrawal RK, Grassucci R, Squires CL, Dahlberg AE, Frank J: **Major rearrangements in the 70S ribosomal 3D structure caused by a conformational switch in 16S ribosomal RNA.** *EMBO J* 1999, **18**:6501-6507.
- The conformational consequences of a specific base pairing change in 16S rRNA are elucidated at intermediate resolution. The change in question is likely to occur with each cycle of peptide chain elongation and is probably related to the proofreading process.
44. Frank J, Zhu J, Penczek P, Li Y, Srivastava S, Verschoor A, Radermacher M, Grassucci R, Lata RK, Agrawal RK: **A model of protein synthesis based on cryo-electron microscopy of the *E. coli* ribosome.** *Nature* 1995, **376**:441-444.
45. Lata KR, Agrawal RK, Penczek P, Grassucci R, Zhu J, Frank J: **Three-dimensional reconstruction of the *Escherichia coli* 30S ribosomal subunit in ice.** *J Mol Biol* 1996, **262**:43-52.
46. Frank J, Agrawal RK: **A ratchet-like inter-subunit reorganization of the ribosome during translocation.** *Nature* 2000, **406**:319-322.
- It is shown that the two ribosomal subunits do indeed move relative to each other during the translocation step of the elongation cycle, as biochemists have long thought probable.
47. Agrawal RK, Spahn CM, Penczek P, Grassucci RA, Nierhaus KH, Frank J: **Visualization of tRNA movements on the *Escherichia coli* 70S ribosome during the elongation cycle.** *J Cell Biol* 2000, **150**:447-460.
- This is the latest contribution of electron microscopists to the still-developing story of how tRNAs interact with the ribosome. It is useful not only for the new information provided, but also because of the analysis of earlier data it provides.
48. Moazed D, Noller HF: **Intermediate states in the movement of transfer RNA in the ribosome.** *Nature* 1989, **342**:142-148.
49. Stark H, Orlova EV, Rinke-Appel J, Junke N, Mueller F, Rodnina M, Wintermeyer W, Brimacombe R, van Heel M: **Arrangement of tRNAs in pre- and posttranslocational ribosomes revealed by electron cryomicroscopy.** *Cell* 1997, **88**:19-28.
50. Rodnina MV, Stark H, Savelsbergh A, Wieden HJ, Mohr D, Matassova NB, Peske F, Daviter T, Gualerzi CO, Wintermeyer W: **GTPases mechanisms and functions of translation factors on the ribosome.** *Biol Chem* 2000, **381**:377-387.
51. Agrawal RK, Penczek P, Grassucci RA, Frank J: **Visualization of elongation factor G on the *Escherichia coli* 70S ribosome: the mechanism of translocation.** *Proc Natl Acad Sci USA* 1998, **95**:6134-6138.
52. Stark H, Rodnina MV, Wieden HJ, van Heel M, Wintermeyer W: **Large-scale movement of elongation factor G and extensive conformational change of the ribosome during translocation.** *Cell* 2000, **100**:301-309.
- A cryo-electron microscopy study of several functional states of EF-G bound to the ribosome. The remarkable changes in EF-G conformation and in the mode of EF-G binding to the ribosome that the authors report are both a challenge to the imagination and a call to action for the other members of the ribosome community.
53. Agrawal RK, Heagle AB, Penczek P, Grassucci RA, Frank J: **EF-G-dependent GTP hydrolysis induces translocation accompanied by large conformational changes in the 70S ribosome.** *Nat Struct Biol* 1999, **6**:643-647.
- This paper provides important information about the structure of the complexes EF-G forms with ribosomes. The results should be compared with those presented in [52\*\*].
54. Wriggers W, Agrawal RK, Drew DL, McCammon A, Frank J: **Domain motions of EF-G bound to the 70S ribosome: insights from a hand-shaking between multi-resolution structures.** *Biophys J* 2000, **79**:1670-1678.
55. Gomez-Lorenzo MG, Spahn CM, Agrawal RK, Grassucci RA, Penczek P, Chakraborty K, Ballesta JP, Lavandera JL, Garcia-Bustos JF, Frank J: **Three-dimensional cryo-electron microscopy localization of EF2 in the *Saccharomyces cerevisiae* 80S ribosome at 17.5 Å resolution.** *EMBO J* 2000, **19**:2710-2718.
56. McCutcheon JP, Agrawal RK, Phillips SM, Grassucci RA, Gerchman SE, Clemons WM Jr, Ramakrishnan V, Frank J: **Location of translational initiation factor IF3 on the small ribosomal subunit.** *Proc Natl Acad Sci USA* 1999, **96**:4301-4306.
57. Carson M: **Ribbons 2.0.** *J Appl Crystallogr* 1991, **24**:958-961.
58. Gutell RR: **Comparative sequence analysis and the structure of 16S and 23S rRNA.** In *Ribosomal RNA. Structure, Evolution, Processing, and Function in Protein Biosynthesis*. Edited by Dahlberg AE, Zimmermann RA. Boca Raton: CRC Press; 1996:111-128.
59. Brodersen DE, Clemons WM, Carter AP, Morgan-Warren RJ, Wimberly BT, Ramakrishnan V: **The structural basis for the action of the antibiotics tetracycline, pactamycin, and hygromycin B on the 30S ribosomal subunit.** *Cell* 2000, **103**:1143-1154.
60. Carter AP, Clemons WM Jr, Brodersen DE, Morgan-Warren RJ, Hartsch T, Wimberly BT, Ramakrishnan V: **Crystal structure of an initiation factor bound to the 30S ribosomal subunit.** *Science* 2001, **291**:498-501